

**Accepted in 'Neuromodulation' – March 21, 2008**

# Closed-Loop Control of FES-Assisted Arm-Free Standing in Individuals with Spinal Cord Injury: A Feasibility Study

Running Title: Closed-Loop Control of FES-Assisted Standing

Authors:

Albert H. Vette<sup>\*,†</sup>, Dipl.-Ing., Kei Masani<sup>\*,†</sup>, Ph.D., Joon-Young Kim<sup>†,‡</sup>, M.A.Sc.,  
and Milos R. Popovic<sup>\*,†</sup>, Ph.D.

Affiliations:

\* Institute of Biomaterials and Biomedical Engineering, University of Toronto,  
164 College Street, Toronto, Ontario, M5S 3G9, Canada

† Toronto Rehabilitation Institute, Lyndhurst Centre,  
520 Sutherland Drive, Toronto, Ontario, M4G 3V9, Canada

‡ Department of Mechanical and Industrial Engineering, University of Toronto,  
5 King's College Road, Toronto, Ontario, M5S 3G8, Canada

Sources of Financial Support:

The International Council for Canadian Studies, the Canadian Institutes of Health Research, the Natural Sciences and Engineering Research Council of Canada, the Canadian Fund for Innovation, the Ontario Innovation Trust, the German National Academic Foundation, and the Tateishi Technology Foundation.

Corresponding Author:

Albert H. Vette, Dipl.-Ing.  
Rehabilitation Engineering Laboratory  
Institute of Biomaterials and Biomedical Engineering, University of Toronto  
69 Walmer Road  
Toronto, Ontario, M5R 2X6, Canada  
Phone: +1-416-964-7145  
Email: a.vette@utoronto.ca  
[www.toronto-fes.ca](http://www.toronto-fes.ca)

## **Closed-Loop Control of FES-Assisted Arm-Free Standing in Individuals with Spinal Cord Injury: A Feasibility Study**

Albert H. Vette, Kei Masani, Joon-Young Kim, and Milos R. Popovic.

### **ABSTRACT**

**Objectives:** The purpose of the present study was to show that the design of a neuroprosthesis for unsupported (arm-free) standing is feasible. We review findings suggesting that a closed-loop controlled functional electrical stimulation (FES) system should be able to facilitate arm-free quiet standing in individuals with spinal cord injury (SCI). Particularly, this manuscript identifies: 1) a control strategy that accurately mimics the strategy healthy individuals apply to regulate the ankle joint position during quiet standing, and 2) the degrees of freedom (DOF) of the redundant, closed-chain dynamic system of bipedal stance that have to be regulated to facilitate stable standing.

**Methods and Results:** First, we utilized a single DOF model of quiet standing (*inverted pendulum*) to analytically identify a proportional and derivative (PD) feedback controller that regulates the ankle torque in a physiological manner despite a long sensory-motor time delay. Second, these theoretical results were experimentally validated by implementing the proposed PD controller to stabilize an individual with SCI during quiet standing. Third, a realistic, three-dimensional dynamic model of quiet standing with twelve DOF was used to determine the optimal combination of the minimum number of DOF that need to be regulated with the PD controller to ensure stability during quiet standing. Finally, perturbation simulations confirmed that the kinematics of this system are similar

to those of healthy individuals during perturbed standing.

**Conclusions:** The presented results suggest that stable standing can be achieved in individuals with SCI by controlling only six DOF in the lower limbs using FES, and that a PD controller actuating these DOF can stabilize the system despite a long sensory-motor time delay. Our finding that not all DOF in the lower limbs need to be regulated is particularly relevant for individuals with complete SCI, since some of their muscles may be denervated or difficult to access.

**KEY WORDS**

Arm-free standing, functional electrical stimulation, multi-body dynamics, neuroprosthesis, PD controller, sensory-motor time delay, spinal cord injury.

## I. INTRODUCTION

It has been suggested that the lost ability of an individual with spinal cord injury (SCI) to stand can be regained by means of functional electrical stimulation (FES) (1-7). Most of the early FES systems that facilitated quiet standing were *open-loop* controlled, i.e., systems that apply predefined stimulation sequences to the legs and the torso (2-4). In recent years, also *closed-loop* control of FES-assisted arm-free standing has been studied, which has become an active research field in rehabilitation engineering (5-7). Despite these important efforts, a neuroprosthesis that uses FES to facilitate the task of unsupported (arm-free) standing in a clinical setting does not exist yet. This is in part due to an insufficient understanding of the control strategy that healthy individuals apply to regulate balance during quiet standing. In particular, it is not known how we compensate for a long sensory-motor time delay as well as system redundancies and double-stance closed-chain dynamics that characterize quiet standing. It therefore needs to be determined: 1) what kind of control strategy healthy individuals may apply to regulate the degrees of freedom (DOF) of the lower limb joints that are responsible for stabilizing the upright body (e.g., the anterior-posterior position of the ankle joints) despite a long sensory-motor time delay, and 2) how many DOF of the redundant, closed-chain dynamic system of quiet standing have to be actively regulated with such a control strategy to ensure stability.

The current manuscript reviews recent findings on the physiological and dynamic mechanisms that are responsible for balance control in healthy

individuals during quiet standing. The five original studies (8-12) have been performed as separate projects of a larger research program, the so-called *neuroprosthesis for standing research program*, in order to establish a foundational knowledge on human balance control. This knowledge has the potential to advance the rehabilitation of people who have difficulties with maintaining balance during quiet standing and to facilitate the development of a neuroprosthesis for standing that could assist individuals with SCI or stroke to stand. Throughout the five original studies, the topic was approached in a bimodal manner that allowed the integration of experimental findings within a theoretical framework.

In the first phase of this large research endeavor, a simplified model of quiet standing, described with a single DOF (*inverted pendulum model*), was utilized to identify control strategies that can regulate the active ankle torque in a physiological manner when a long sensory-motor time delay is present (8,9). Note that the ankle joint was chosen for this objective as it is the joint that is most remote from the central nervous system and therefore experiences the longest sensory-motor time delay. In the second phase, the theoretical results from the first phase were experimentally validated by utilizing the proposed controller to regulate the ankle joints of an individual with SCI, showing that the system behaves in a similar manner as the system in healthy individuals (10). Finally, a realistic, three-dimensional dynamic model of quiet standing with twelve DOF was developed to determine the optimal combination of the minimum number of DOF that need to be regulated by the proposed controller to ensure asymptotic

stability of the system (11,12).

By putting the obtained results into a broader perspective, the particular objective of the present review is to provide strong evidence that arm-free quiet standing via FES is, in fact, feasible.

---

## II. GAIN IDENTIFICATION FOR THE PROPOSED CONTROLLER

### A. Methods

#### Simulations

Fig. 1 shows a schematic representation of the modeled system in which the ankle joint position is regulated by a proportional and derivative (PD) controller that approximates the physiological control mechanism at the higher neural level (motor cortex). The body dynamics and kinematics during quiet stance were described using a validated inverted pendulum model (13) with the parameters of a typical adult male (body mass:  $m = 76$  kg; body inertia about the ankle joint during quiet standing:  $I = 66$  kg·m<sup>2</sup>; and height of the body's center of mass above the ankle joint:  $h = 0.87$  m). The input to the body model, i.e., the command torque  $T_c$ , was the total torque exerted about the ankle joint.

The modeled system included three time delays that have been considered in the physiological system of quiet standing (Fig. 1): 1) a feedback time delay representing cumulative time loss due to neural transmission from the ankle somatosensory system to the brain ( $\tau_F$ ); 2) a motor command time delay representing the time loss due to the sensory-motor information process in the central nervous system (CNS) and the neural transmission from the CNS to the plantar flexors<sup>1</sup> ( $\tau_M$ ); and 3) an electromechanical time delay representing the time difference between the moment when the electromyogram (EMG) of the plantar flexors is detected and the moment when the force occurs ( $\tau_E$ ). While  $\tau_F = 40$  ms

---

<sup>1</sup> Since the COM is located *in front of* the ankle joint during quiet standing (14), plantar flexors are continuously activated during quiet standing in order to prevent the body from falling forward. Dorsiflexors on the other hand are silent or only intermittently active.

and  $\tau_E = 10$  ms were assumed to be constant in the simulations (15,16),  $\tau_M$  was introduced as a variable as there is no consensus in the literature on how long it actually is (9).

In order to mimic quiet standing as close as possible, a random disturbance torque ( $T_d$ ) to the ankle joint was included (Fig. 1), which corresponded to the summation of all internal noise inducing spontaneous body sway.  $T_d$  was produced as a low-pass filtered, uniform random number with zero mean and unity variance. The random number was generated with a sample time of 0.1 s and filtered by a first-order filter with a cutoff frequency of 5 Hz. The maximum amplitude of  $T_d$  was approximately  $\pm 2.0$  Nm, which is equivalent to the ankle moment generated when manipulating an object of approximately 0.2 to 0.3 kg with fully extended arms. It should also be noted that this noise had similar amplitude and frequency components as the one used for weak external perturbations in the study by Fitzpatrick *et al.* (17).

Simulations of the model were performed to calculate the center of mass (COM) position and velocity as well as the neural motor command at the plantar flexors ( $M_C$ ) as a function of time. Linear control theory and cross-correlation analysis (CCF) were used to identify proportional ( $K_P$ ) and derivative ( $K_D$ ) gain pairs for the PD controller that: 1) ensured a stable and robust system behavior; and 2) evoked body sway characteristics similar to those observed in experiments with able-bodied subjects (8).

#### PD Gain Identification Procedure

In a first step of the PD gain identification procedure,  $K_P$ - $K_D$ - $\tau_M$  sets were

---

identified for which the system satisfied Nyquist's stability criterion and at the same time exhibited a predefined level of robustness. This additional constraint was necessary since the inverted pendulum model represented a simplified description of the body during quiet standing, and parameters, such as the COM location and body segment lengths, are always modeled with a certain degree of inaccuracy. Therefore,  $K_P$ - $K_D$ - $\tau_M$  sets that did not produce an open-loop response with a phase margin of at least  $20^\circ$  as well as a gain margin of  $-1$  dB were not considered as sufficiently robust. These choices for the minimum phase and gain margin are used extensively in the analysis of feedback systems, for which the reference signal is constant and the dynamic behavior of the system influenced by a noise signal between the controller and the plant (18).

In a second step, the dynamics of the modeled system were captured by the time shifts between the motor command and the body kinematics (position and velocity) and compared with those of healthy individuals. For these control subjects, the time shifts were calculated from two CCFs (8): 1) CCF between the COM position ( $COM_{POS}$ ) and the EMG of the right medial gastrocnemius muscle ( $M_{EMG}$ ); and 2) CCF between the COM velocity ( $COM_{VEL}$ ) and  $M_{EMG}$ . The resulting time shifts were defined as the objective time shifts for the CCF comparison.

The time shift from  $COM_{POS}$  to  $M_{EMG}$  is defined by the lag time of the peak of the CCF between  $COM_{POS}$  and  $M_{EMG}$ . The resulting group average value  $\pm$  SD from our previous study (8) was  $-155 \pm 46$  ms, which indicates that  $M_{EMG}$  preceded  $COM_{POS}$ . This time shift range was defined as the objective range  $TS_{POS}$ .

for the CCF between  $COM_{POS}$  and the motor command  $M_C$  as calculated by the PD controller in the simulations. The CCF between  $COM_{VEL}$  and  $M_{EMG}$  had two peaks: one with a positive time shift and the other one with a negative time shift. According to the experimental results, the positive time shift was  $121 \pm 134$  ms and the negative time shift was  $-620 \pm 134$  ms. These two time shift ranges were defined as the objective ranges  $TS_{VEL}$  for the CCF between  $COM_{VEL}$  and the motor command  $M_C$  in the simulations. The comparison of the time shifts obtained in the simulations with  $TS_{POS}$  and  $TS_{VEL}$  finally allowed us to identify PD control gain pairs for which the stable system exhibited the same system dynamics as observed in healthy individuals during quiet standing.

## ***B. Results***

The pool of PD gains that satisfied the above criteria is depicted in Fig. 2. The described gains ensured a robust system behavior with the required physiological dynamics and compensated for the sensory-motor time delay by producing a motor command that sufficiently preceded body sway. Note that the  $K_P/K_D$  ratio of the determined gain combinations was in the range of 1.45 to 3.83, which is much smaller than the range commonly used for position control of dynamic systems. Thus, it was concluded that the CNS might adopt a control strategy that relies considerably on the body's velocity information. The largest  $\tau_M$  for which the PD controller produced a robust and physiological system behavior was 85 ms. The gains that stabilized the system up to a  $\tau_M$  of 85 ms, i.e., a total time delay of 135 ms, were  $K_P = 750 \text{ Nm}\cdot\text{rad}^{-1}$  and  $K_D = 350 \text{ Nm}\cdot\text{s}\cdot\text{rad}^{-1}$ .

A detailed account of this section is given in Masani *et al.* (8,9).

---

### III. EXPERIMENTAL VALIDATION OF THE PROPOSED PD CONTROLLER

#### A. *Methods*

##### Experimental Setup

Fig. 3 shows a schematic of the experimental setup: The PD controlled system received its input from a laser sensor (Keyence, Japan), which recorded the anterior-posterior fluctuation of the approximated COM. Using these measurements, the controller calculated the active ankle torque required to stabilize the system. After dividing the torque into equal portions for each leg, an electrical stimulator (Compex Motion, Switzerland) provided the stimulation command ( $M_{\text{STIM}}$ ) for both plantar flexors. The stimulation pulses had a constant frequency (35 Hz) and pulse duration (300  $\mu\text{s}$ ), and regulated the muscle contractions via amplitude variation (mA). Note that the stimulation amplitude versus torque relationship of the subject's plantar flexors was determined in a preliminary experiment. In addition to the COM measurements, a force plate (Kistler, Switzerland) was used to determine the center of pressure (COP) fluctuation of the subject. While only the COM was used for balance control, both COM and COP were subject to the stability analysis.

The kernel that implemented the identified PD controller (Visual C++ 5.0, Microsoft, USA) consisted of the following main components:

- Butterworth 3<sup>rd</sup> order low-pass filter with 10 Hz cut-off frequency that eliminated measurement noise (19).
- PD controller with gains of  $K_P = 750 \text{ Nm}\cdot\text{rad}^{-1}$  and  $K_D = 350 \text{ Nm}\cdot\text{s}\cdot\text{rad}^{-1}$  (9).

- Maximum limit for torque generation (26 Nm per leg) as seen in experiments with healthy subjects (20).

It should be emphasized that the feedback system's closed-loop time delay of 85 ms was within the range of the sensory-motor time delay of healthy individuals (9).

### Subject

The proposed system was tested with a male subject that had difficulty maintaining balance during quiet standing due to a neurological disorder called von Hippel-Lindau Syndrome (VHL). VHL is a rare genetic multi-system disorder characterized by the abnormal growth of tumors in certain parts of the body including the CNS. The subject was 36 years of age, had height 173 cm, mass 59 kg, and experienced VHL from birth on. At the time of study, he had partial loss of sensation, proprioception and motor control caused by various tumors in the cerebellum, the medulla, and the spinal cord. As the subject suffered under more severe neurological deficits and required two canes for walking, he was functioning at a Grade III level on the modified McCormick scale (21).

### Stability Analysis

In order to determine the effectiveness of the PD controller to facilitate quiet standing, the subject's performance was compared for three treatments:

- NOstim: Trials without stimulation (0 mA)
- CONSTstim: Trials with constant stimulation (33 mA per leg)
- PDstim: Trials with PD controlled stimulation (30-38 mA per leg with a resultant mean of approximately 33 mA).

For every treatment, three trials of 140 s each were recorded. In each trial, the subject was asked to stand still and maintain balance with eyes open, i.e., the eye condition present during activities of daily living. The COM and COP time series were logged at a sampling frequency of 1 kHz and low-pass filtered using a fourth order, zero phase-lag Butterworth filter with a cutoff frequency of 5 Hz (22). The latter 120 s of the recordings were divided into two time series of 60 s each (23) and quantified using measures of postural steadiness (22): 1) Distance measures (MDIST: mean distance, RDIST: root mean square distance, and RANGE); and 2) Velocity measures (MVELO: mean velocity and RVELO: root mean square velocity). Finally, the identified measures were analyzed by means of a one-way ANOVA with a significance level of  $\alpha = 0.05$ .

#### Cross-Correlation Analysis

Similar to the simulations, the subject's COM– $M_{\text{STIM}}$  dynamics during the PDstim trials were compared with the ones of healthy individuals by means of CCF analysis. Using the pre-processed COM and  $M_{\text{STIM}}$  data, two CCFs were calculated: 1) CCF between  $\text{COM}_{\text{POS}}$  and  $M_{\text{STIM}}$ ; and 2) CCF between  $\text{COM}_{\text{VEL}}$  and  $M_{\text{STIM}}$ . Again, the average time shifts from  $\text{COM}_{\text{POS}}$  to  $M_{\text{STIM}}$  and from  $\text{COM}_{\text{VEL}}$  to  $M_{\text{STIM}}$  were related to  $\text{TS}_{\text{POS}}$  and  $\text{TS}_{\text{VEL}}$ , respectively (see *PD Gain Identification Procedure*). Comparing the CCFs of the PDstim trials with these target ranges allowed us to evaluate whether the PD controller can generate body dynamics as seen in healthy individuals (8) and the simulations (9).

#### **B. Results**

The results of the COM and COP stability analysis are shown in Table 1.

The PDstim trials had the smallest average value (bold) for all COM measures, with differences between treatments being statistically significant (\*) for all measures except RANGE. The COP analysis on the other hand revealed that the distance measures were smallest for PDstim, whereas the velocity measures were smallest for NOstim and largest for PDstim. The group differences were statistically significant for the COP distance but not the COP velocity measures.

Fig. 4a shows the average CCFs between  $COM_{POS}$  and  $M_{STIM}$  (left) and between  $COM_{VEL}$  and  $M_{STIM}$  (right) for each of the six PDstim recordings. The bold black curves indicate the group average CCFs for all recordings, whereas the gray vertical lines mark the target ranges  $TS_{POS}$  and  $TS_{VEL}$ . It can be seen that the peaks of the average CCFs (one for  $COM_{POS}-M_{STIM}$  and two for  $COM_{VEL}-M_{STIM}$ ) lie within the specified target ranges. For comparison, respective CCFs of a single able-bodied subject from (8) are shown in Fig. 4b (five trials of 30 s each).

A detailed account of this section is given in Vette *et al.* (10).

---

## IV. STABILIZATION OF A REALISTIC DYNAMIC MODEL OF QUIET STANCE

### A. *Methods*

#### Three-Dimensional Dynamic Model and Active DOF Determination

Since the PD controller has been shown to be effective in maintaining stability during quiet stance by regulating the ankle joint, the next objective was to use the same control strategy for stabilization of a *realistic* dynamic model of quiet standing. The three-dimensional (3D) model with twelve DOF, which was developed to represent the human body during quiet stance, is shown in Fig. 5. The head-arms-trunk complex (HAT) was represented as a single rigid body with a constant mass and moment of inertia. Each leg consisted of six DOF (total of twelve DOF), which has been shown to be a sufficient approximation of the double-support (i.e., bipedal) characteristics of quiet stance (24). The feet were not included in the model since it was assumed that they were fully in contact with the ground. The DOF of the joints were as follows: ankle inversion/eversion ( $lA_{IE}$ ,  $rA_{IE}$ ); ankle dorsiflexion/plantarflexion ( $lA_{DP}$ ,  $rA_{DP}$ ); knee flexion/extension ( $lK_{FE}$ ,  $rK_{FE}$ ); hip abduction/adduction ( $lH_{AA}$ ,  $rH_{AA}$ ); hip flexion/extension ( $lH_{FE}$ ,  $rH_{FE}$ ); and hip rotation ( $lH_{RT}$ ,  $rH_{RT}$ ). Denavit-Hartenberg notation was used for kinematic modeling, and Newton-Euler and Lagrange formulations were applied to the HAT and the legs, respectively, to obtain the dynamic model of the system.

In order to identify the minimum number of DOF that need to be controlled to stabilize the model in Fig. 5, i.e., the minimum active DOF, *Nakamura's inverse method* was used (25). It revealed that, as long as the number

of the active DOF is equal or greater than six and the rank of the Jacobian matrix with respect to the passive DOF is equal to six, the inverse dynamics solution exists (11). Table 2 shows six combinations of six active DOF combinations (6-DOF) for which the passive Jacobian matrix had a full rank for all feasible postures and motions during quiet standing. Note that the six cases of 6-DOF in Table 2 assume  $l_{A_{IE}}$ ,  $r_{A_{IE}}$ ,  $l_{H_{RT}}$ , and  $r_{H_{RT}}$  to always be passive DOF as they are difficult to actuate with contemporary transcutaneous FES technology (7).

#### Identification of Optimal 6-DOF Combination

After discovering that six 6-DOF combinations exist for which the system can be stabilized, the next objective was to identify a potentially optimal 6-DOF combination, i.e., a combination that required minimum joint torques for all perturbation directions (D1–D8 in Fig. 5). For this purpose, the joint torques of all six 6-DOF combinations were estimated using the inverse dynamics method and body kinematics of four healthy individuals during perturbed arm-free standing. The subjects had an age between 31 and 32 years and were initially standing quietly with their eyes closed and their arms folded on the chest. They were then perturbed at their COM using an impulse-like force of 45 N acting in one of the eight perturbation directions. During the experiments, a motion analysis system (Optotrak 3020, Northern Digital, Canada) recorded the joint angles of the body segments, which were used to calculate the angular velocities and accelerations via the *finite differentiation technique* (19). The lengths of the body segments of each subject were measured before the experiments, whereas the mass, the moment of inertia, and the location of the COM of each body segment were

estimated based on the subject's anthropometric data (19). Using the kinematic data and the anthropometric parameters, the joint torques were calculated with the inverse dynamics method for all eight perturbation directions and all 6-DOF combinations (Table 2).

Finally, a norm based measure for each active DOF's torque profile was determined by numerically integrating the norm of the torque as a function of time over an interval of five seconds, i.e.,  $\int_0^5 |\tau_a| dt$  (Nm·s). Note that  $\tau_a$  is one active DOF's mean torque as a function of time obtained from three perturbation experiments per direction and subject. The value of  $\int_0^5 |\tau_a| dt$  is referred to in the paper as *torque sum*. The estimation of the *overall* torque sum for each case of 6-DOF allowed us to identify the optimal 6-DOF combination, i.e., the combination that exhibits the minimum torque sum for all six active DOF among the 6-DOF.

### Stability Analysis of Proposed FES Control Strategy

Based on the results of the previous sections, a PD plus gravity compensator for the control of FES-assisted arm-free standing was proposed. Note that the gravity compensator counteracts the forces generated by gravity, whereas the PD component of the controller minimizes the error between the desired and the actual states of the system. The proposed control scheme used  $K_P$  and  $K_D$  gains determined in Section II (9) and regulated the optimal 6-DOF of the dynamic model in Fig. 5. In a first step of the stability analysis, a Lyapunov function was identified to prove that the system with PD and gravity compensation is asymptotically stable in large, i.e., for all states. In a second step,

simulations were performed to determine the system dynamics for this control scheme. The model represented an individual with complete SCI whose weight and height were 66.7 kg and 1.72 m, respectively. Furthermore, the individual with SCI was assumed to be initially in the upright posture. The model was perturbed by a sudden external force of 100 N, which acted on the COM of the HAT. Note that the gravity effects of the head and arm motion were considered as additional external disturbances. As a result, an external force of  ${}^wF_o = [-70.71 \ 0 \ -70.71 \ 10 \ 10 \ 10]^T$  (N, Nm) was applied for 0.5 s during the simulation. The gains of the PD plus gravity compensator, chosen according to Section II (9), were  $K_P = 1000 \text{ I Nm}\cdot\text{rad}^{-1}$  and  $K_D = 300 \text{ I Nm}\cdot\text{s}\cdot\text{rad}^{-1}$ .

## ***B. Results***

The inverse dynamics method revealed that the recorded body kinematics could be generated by physiologically feasible joint torques for all six cases of six active DOF (6-DOF). In Fig. 6, the overall torque sums at all active DOF calculated for all eight directions of perturbation (D1-D8 in Fig. 5) and all six 6-DOF combinations (Table 2) are presented. Cases V and VI generated the lowest overall torque sum at all six active DOF for all directions of perturbation. Cases I and II generated the largest overall torque sum at all active DOF for the forward perturbations (D1, D2, and D8), whereas Cases III and IV generated the largest overall torque sum at all active DOF for the backward perturbations (D4, D5, and D6). As a result, Cases V and VI proved to be the optimal 6-DOF combinations as they required the minimum joint torques for body stabilization, and this for all perturbation directions.

The performed Lyapunov stability analysis revealed that the system was asymptotically stable when controlled by the proposed PD plus gravity compensator. Note that this was true for all six 6-DOF combinations, i.e., for Cases I to VI. In order to stabilize the perturbed model in the simulations, the DOF of Case VI were chosen to be regulated by the PD plus gravity compensator as Cases V and VI generated the minimum torque in the inverse dynamics analysis among the six 6-DOF cases. As seen in Fig. 7, the body returned to the initial upright posture in about 2 s after the external disturbance was applied.

A detailed account of this section is given in Kim *et al.* (11,12).

## V. DISCUSSION

### A. *Controller to be Used – Single DOF Control Strategy*

The theoretical study of Section II suggests that a PD control strategy can theoretically mimic the physiological controller as determined by the CCF analysis and regulate the anterior-posterior ankle joint angle (single DOF) during quiet standing. It has to be emphasized that the closed-loop feedback model was found to be stable and robust for a wide range of PD gains. Note that this was even true in the presence of a long sensory-motor time delay, an outcome that has been considered as unfeasible in the past. As such, the PD controller represents a valid candidate for regulating a single DOF during quiet standing, in particular the anterior-posterior ankle joint position.

The theoretical results were further supported by findings obtained from the experiments with an individual with SCI (Section III). In fact, if the PD controller identified in Section II is used in combination with an FES system to stabilize the ankle joint (dynamic stimulation), the COM measures as well as the COP distance measures during standing were smallest when compared to constant or no stimulation. This additionally implies that FES has the ability to effectively translate a given motor command fluctuation into a desired level of ankle torque fluctuation.

In accordance with the theoretical PD gain selection procedure (Section II), the experiments of Section III also revealed that the time advance of the motor command  $M_{\text{STIM}}$  with respect to body sway (193 ms) was within the specified target range of healthy individuals ( $155 \pm 46$  ms). As such, the implemented PD

controller is, in fact, capable of providing a motor command that sufficiently precedes body sway in spite of the closed-loop time delay. Note that the time advance of  $M_{\text{STIM}}$  is fairly large in comparison with healthy individuals, implying that even more severe control demands, e.g., a longer time delay in the feedback loop, can be handled. Taking furthermore into account that also the COM velocity exhibited a physiological behavior (since the peaks of the CCF between  $\text{COM}_{\text{VEL}}$  and  $M_{\text{STIM}}$  were within the specified target ranges), it can be concluded that  $M_{\text{STIM}}$  generated dynamics as seen in healthy subjects.

The findings from Sections II and III on the single DOF control strategy demonstrate that a PD controller represents a valid candidate for regulating particular DOF when developing an FES system for arm-free standing in individuals with SCI. It has also to be noted that the control system's robustness as well as its use of body kinematics to generate an appropriate motor command are key features of biological control systems. While these findings do not imply that the CNS actually applies a PD-like control strategy to regulate balance, one cannot ignore the possibility that it is at least theoretically possible.

### ***B. DOF to be Controlled – System Control Strategy***

One of the most significant results obtained from the project described in Section IV is the fact that not all twelve, but only six DOF in the lower limbs of a standing human have to be actuated to ensure asymptotic stability against external perturbations. Moreover, we identified the *optimal* cases among the 6-DOF combinations such that the overall torque sum was lowest and most evenly distributed among the two legs for all eight directions of perturbation. The

optimal combinations, Cases V and VI in Table 2, consisted of one  $H_{AA}$ , one  $H_{FE}$ , two  $K_{FE}$ , and two  $A_{DP}$ . These two cases actually imply four different optimal combinations as each case in Table 2 has a mirror image due to the symmetry of the two legs. Cases I to IV on the other hand had two  $H_{FE}$ , thus missing one anterior-posterior DOF to be actuated in either the ankle or knee joint. It has to be noted that the joint torque patterns of Cases V and VI were fundamentally different from those of the other four cases: For the optimal combinations, the torques of all the active anterior-posterior DOF acted together in the same direction, whereas in the other four cases at least one DOF existed that was actuated in the opposite direction to account for the existence of passive DOF in the closed-chain dynamic system. Since this was not necessary for Cases V and VI, it is plausible that these two cases require less amount of torque compared to the other four cases.

To ensure the feasibility of an actual FES system that has to regulate the six active DOF of Cases V and VI, it had to be investigated whether the required torque levels can actually be generated by means of FES. This was confirmed exemplarily for the two anterior-posterior and medial-lateral DOF that exhibited the largest torque levels during all perturbations. The particular torque peaks, which occurred at  $A_{DP}$  (33 Nm of plantar flexion) and at  $H_{AA}$  (90 Nm of abduction) during the D1 and D3 perturbations, respectively, have been shown to be producible by contemporary surface FES technology (10, 26).

Another important result of this project is the fact that the PD controller, which was identified and validated using a single DOF, can stabilize the three-

dimensional model against realistic external perturbations. After demonstrating by means of the Lyapunov analysis that *asymptotic* stability can be obtained with the PD plus gravity compensator by regulating only six out of the model's twelve DOF, the perturbation simulations not only confirmed the stability of the system, but also revealed kinematics similar to those of healthy individuals during perturbed standing.

Although these findings clearly demonstrate that six active DOF are theoretically sufficient to stabilize the body during perturbed stance, it is possible that in a practical application more than six DOF will be actuated (e.g., symmetrical combination of eight active DOF). Future experiments with individuals with SCI will be performed to experimentally validate whether six active DOF are, in fact, sufficient to regulate balance during stance or whether the actuation of additional DOF is required.

### ***C. Limitations***

Despite the reported progress towards the development of a neuroprosthesis for arm-free standing in individuals with SCI, many other challenges need yet to be addressed. These include the implementation of a sensor for measuring balance and the prevention of foot movement during standing, the reduction of FES induced muscle fatigue, and the selection of the muscles that need to be actuated by means of FES to generate the required joint (DOF) torques. The last challenge is additionally complicated by the fact that some of the targeted muscles are actually two-joint muscles, making the regulation of particular DOF more complex. Our team and many others are currently attempting to address

these and other issues that stand in the way of the development and implementation of a reliable and efficient system for FES-assisted standing.

## VI. CONCLUSION

This review integrates recent findings that are crucial for understanding the control strategy healthy individuals apply to compensate for a long sensory-motor time delay as well as system redundancies and double-stance closed-chain dynamics that characterize quiet standing. Some of these challenges, although most critical for the success of FES systems for arm-free standing in individuals with SCI, have often been neglected in the past. The presented work provides some answers to these challenging problems and suggests potent solutions that are based on theoretical and experimental findings. We are hopeful that these findings will assist the FES community in developing the first clinically viable FES system for arm-free standing. In particular, the present study outlines a well-defined procedure that could be used to develop a neuroprosthesis for standing: 1) find a combination of six DOF that can be actuated using FES such that it belongs to the sets of 6-DOF presented in Table 2; 2) determine whether the torques required at each active DOF can be generated using contemporary FES technology; and 3) implement PD plus gravity compensators in combination with the FES system to regulate the 6-DOF combination identified in 1). Our finding that not all DOF in the lower limbs need to be regulated or even activated is particularly relevant for individuals with complete SCI, since some of their muscles may be denervated or difficult to access. Moreover, this also implies that a 12-channel FES system (two channels per active DOF) is sufficient to regulate balance during quiet stance. In other words, a less complex and therefore more reliable FES system is required to implement a neuroprosthesis for arm-free standing than previously believed.

**REFERENCES**

1. Jaeger RJ. Design and simulation of closed-loop electrical stimulation orthoses for restoration of quiet standing in paraplegia. *J Biomech* 1986;19:825-835.
2. Kralj A, Bajd T, Turk R, Benko H. Posture switching for prolonging functional electrical stimulation standing in paraplegic patients. *Paraplegia* 1986;24:221-230.
3. Kralj A, Bajd T. *Functional electrical stimulation: Standing and walking after spinal cord injury*. Boca Raton, FL: CRC Press, 1989.
4. Veltink PH, Donaldson N. A perspective on the control of FES supported standing. *IEEE Trans Rehab Eng* 1998;6:109-112.
5. Matjačić Z, Bajd T. Arm-free paraplegic standing. I. Control model synthesis and simulation. *IEEE Trans Rehab Eng* 1998;6:125-138.
6. Holderbaum W, Hunt KJ, Gollee H.  $H_{\infty}$  robust control design for unsupported paraplegic standing: experimental evaluation. *Control Eng Practice* 2002;10:1211-1222.
7. Gollee H, Hunt KJ, Wood DE. New results in feedback control of unsupported standing in paraplegia. *IEEE Trans Neural Sys Rehab Eng* 2004;12:73-80.
8. Masani K, Popovic MR, Nakazawa K, Kouzaki M, Nozaki D. Importance of body sway velocity information in controlling ankle extensor activities during quiet stance. *J Neurophysiol* 2003;90:3774-3782.
9. Masani K, Vette AH, Popovic MR. Controlling balance during quiet standing: Proportional and derivative controller generates preceding motor command to body sway position. *Gait and Posture* 2006;23:164-172.
10. Vette AH, Masani K, Popovic MR. Implementation of a physiologically identified PD feedback controller for regulating the active ankle torque during quiet stance. *IEEE Trans Neural Sys Rehab Eng* 2007;15:235-243.

11. Kim JY, Popovic MR, Mills JK. Dynamic modeling and torque estimation of FES-assisted arm-free standing for paraplegics. *IEEE Trans Neural Sys Rehab Eng* 2006;14:46-54.
12. Kim JY, Mills JK, Vette AH, Popovic MR. Optimal combination of minimum degrees of freedom to be actuated in the lower limbs to facilitate arm-free paraplegic standing. *ASME J Biomech Eng* 2007;129:838-847.
13. Gage WH, Winter DA, Frank JS, Adkin AL. Kinematic and kinetic validity of the inverted pendulum model in quiet standing. *Gait and Posture* 2004;19:124-132.
14. Smith JW. The forces operating at the human ankle joint during standing. *J Anat* 1957;91:545-564.
15. Applegate C, Gandevia SC, Burke D. Changes in muscle and cutaneous cerebral potentials during standing. *Exp Brain Res* 1988;71:183-188.
16. Isabelle M, Sylvie Q-B, Chantal P. Electromechanical assessment of ankle stability. *Eur J Appl Physiol* 2003;88:558-564.
17. Fitzpatrick R, Burke D, Gandevia C. Loop gain of reflexes controlling human standing measured with the use of postural and vestibular disturbances. *J Neurophysiol* 1996;76:3994-4008.
18. Unbehauen H. *Control systems – classical methods for analysis and synthesis of linear and continuous control systems and fuzzy control systems*. Wiesbaden, Germany: Vieweg, 2002.
19. Winter DA. *Biomechanics and motor control of human movement*. New York, NY: Wiley & Sons, 1990.
20. Loram ID, Lakie M. Human balancing of an inverted pendulum: Position control by small, ballistic-like, throw and catch movements. *J Physiol* 2002;540:1111-1124.
21. Van Velthoven V, Reinacher PC, Klisch J, Neumann HP, Gläser S. Treatment of intramedullary hemangioblastomas, with special attention to von

Hippel-Lindau disease. *J Neurosurg* 2003;53:1306-1314.

22. Prieto E, Myklebust JB, Hoffmann RG, Lovett EG, Myklebust BM. Measures of postural steadiness: Differences between healthy young and elderly adults. *IEEE Trans Biomed Eng* 1996;43:956-966.

23. Carpenter MG, Frank JS, Winter DA, Peysar GW. Sampling duration effects on centre of pressure summary measures. *Gait and Posture* 2001;13:35-40.

24. Sias FR, Zheng YF. How many degrees-of-freedom does a biped need? *Proc IROS '90, IEEE Int Workshop on Intelligent Robotics and Systems* 1990;1:297-302.

25. Nakamura Y, Ghodoussi M. Dynamics computation of closed-link robot mechanisms with nonredundant and redundant actuators. *IEEE Trans Robotics and Automation* 1989;5:294-302.

26. Marsolais EB, Kobetic R. Development of a practical stimulation system for restoring gait in the paralyzed patient. *Clin Orthop Rel Res* 1988;233:64-74.

Table 1. Comparison of Average Stability Results for Each Treatment. Reprinted from (10), with permission from the Institute of Electrical and Electronics Engineers (© 2007 IEEE).

	<b>COM</b>	<b>NOstim</b>	<b>CONSTstim</b>	<b>PDstim</b>
<b>1)</b>	MDIST* [cm]	0.832 ± 0.166	1.052 ± 0.243	<b>0.690 ± 0.154</b>
	RDIST* [cm]	1.083 ± 0.231	1.253 ± 0.269	<b>0.871 ± 0.217</b>
	RANGE [cm]	6.003 ± 1.382	5.701 ± 1.194	<b>4.498 ± 1.030</b>
<b>2)</b>	MVELO* [cm/s]	0.939 ± 0.115	0.882 ± 0.102	<b>0.776 ± 0.086</b>
	RVELO* [cm/s]	1.237 ± 0.152	1.131 ± 0.136	<b>1.019 ± 0.091</b>
	<b>COP</b>	<b>NOstim</b>	<b>CONSTstim</b>	<b>PDstim</b>
<b>1)</b>	MDIST* [cm]	1.009 ± 0.136	1.158 ± 0.229	<b>0.857 ± 0.126</b>
	RDIST* [cm]	1.308 ± 0.181	1.423 ± 0.270	<b>1.095 ± 0.169</b>
	RANGE* [cm]	8.399 ± 0.898	7.767 ± 1.390	<b>6.723 ± 0.862</b>
<b>2)</b>	MVELO [cm/s]	<b>2.607 ± 0.444</b>	2.691 ± 0.478	2.759 ± 0.740
	RVELO [cm/s]	<b>3.542 ± 0.550</b>	3.582 ± 0.608	3.761 ± 1.099

1) represent distance measures, 2) represent velocity measures.

Table 2. Six Cases of Six Active DOF Combinations. Reprinted from (11), with permission from IEEE (© 2006 IEEE).

	Ankle		Knee		Hip			
	$rA_{DP}$	$lA_{DP}$	$rK_{FE}$	$lK_{FE}$	$rH_{AA}$	$lH_{AA}$	$rH_{FE}$	$lH_{FE}$
<b>I</b>		•	•	•		•	•	•
<b>II</b>	•		•	•		•	•	•
<b>III</b>	•	•		•		•	•	•
<b>IV</b>	•	•	•			•	•	•
<b>V</b>	•	•	•	•	•		•	
<b>VI</b>	•	•	•	•		•	•	

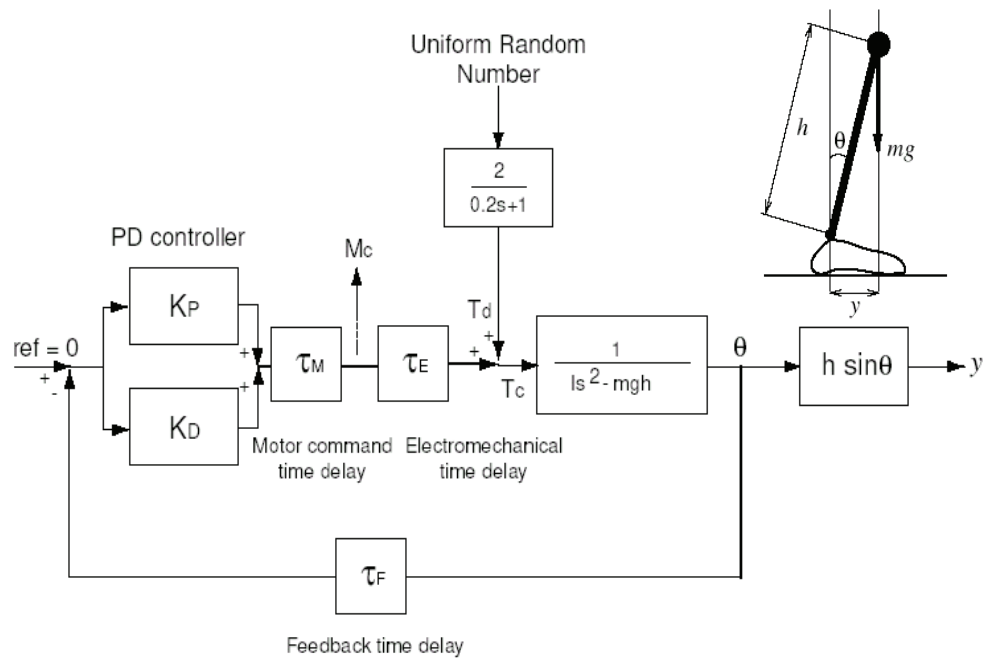


Fig. 1. Inverted pendulum model and closed-loop control scheme of quiet stance.  $y$  is the horizontal COM position,  $h$  the distance of the COM to the ankle,  $\theta$  the body sway angle,  $g$  is the acceleration due to gravity,  $M_C$  is the neural motor command at the plantar flexors, and  $T_c$  the total torque about the ankle. Reprinted from (9), with permission from Elsevier (© 2005 Elsevier).

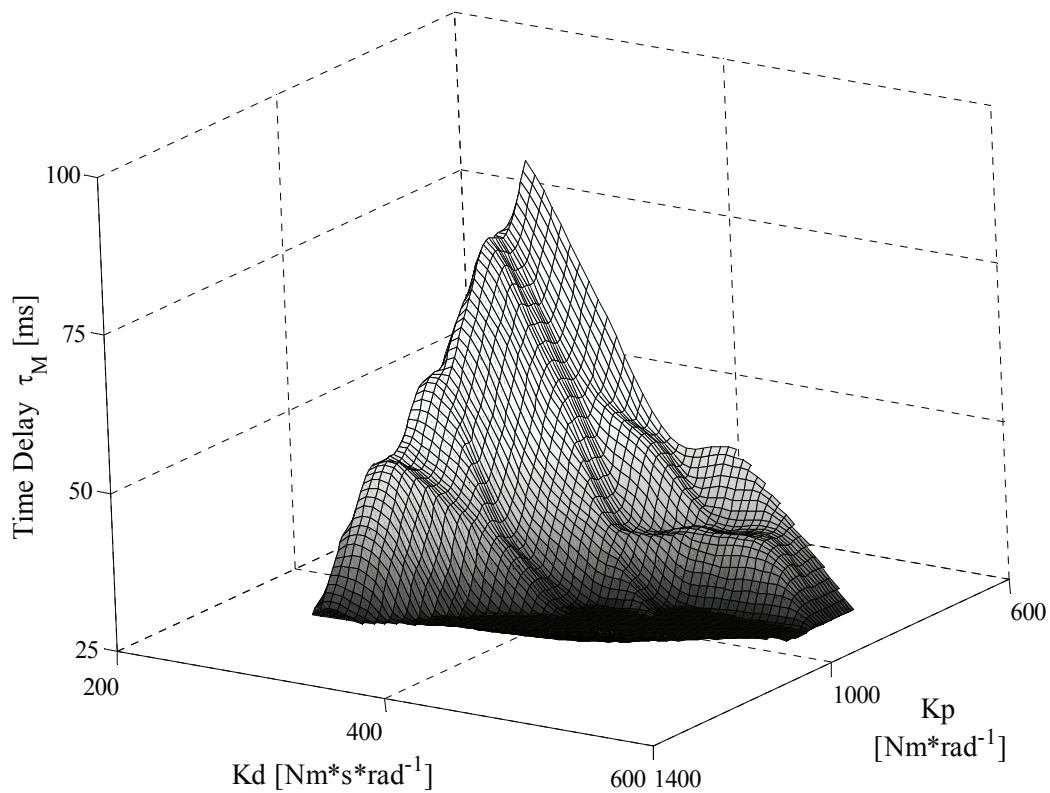


Fig. 2. Pool of PD gains that ensured a stable and robust system with physiological dynamics. It should be noted that the space consists of dots that were interpolated to allow the volume visualization. Reprinted from (9), with permission from Elsevier (© 2005 Elsevier).

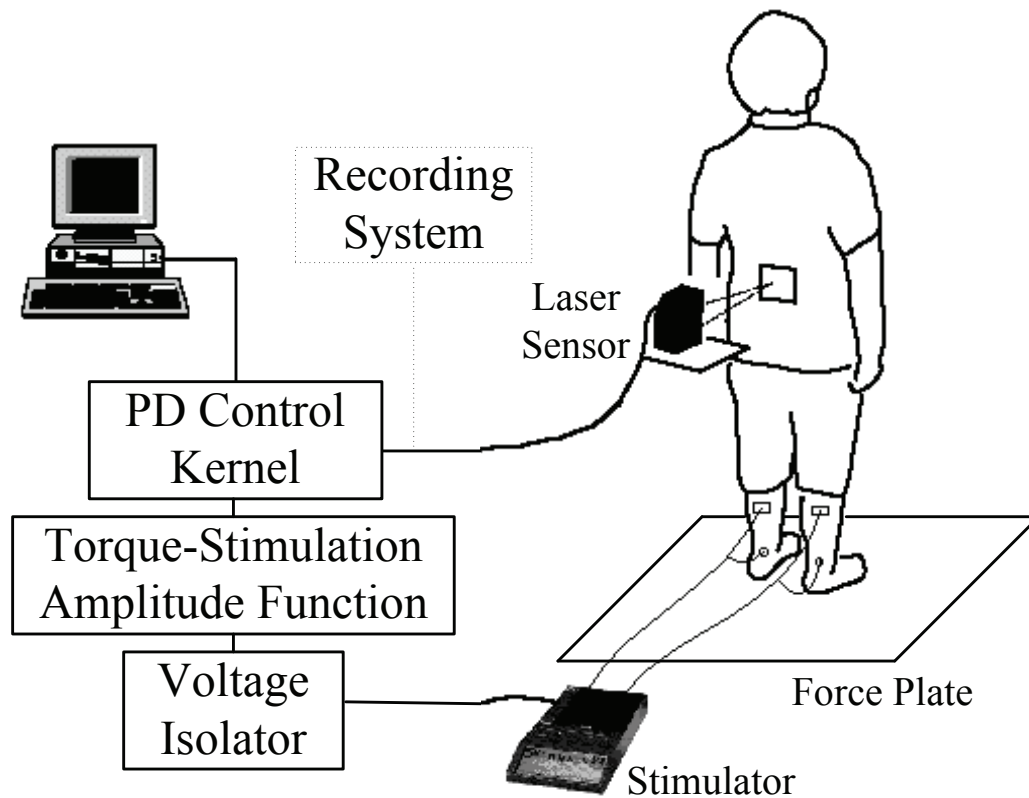


Fig. 3. Schematic of the experimental setup. The laser measurements capturing the fluctuation of spontaneous body sway were sent to the controller, which determined the level of active ankle torque that was needed to stabilize the system. Reprinted from (10), with permission from IEEE (© 2007 IEEE).

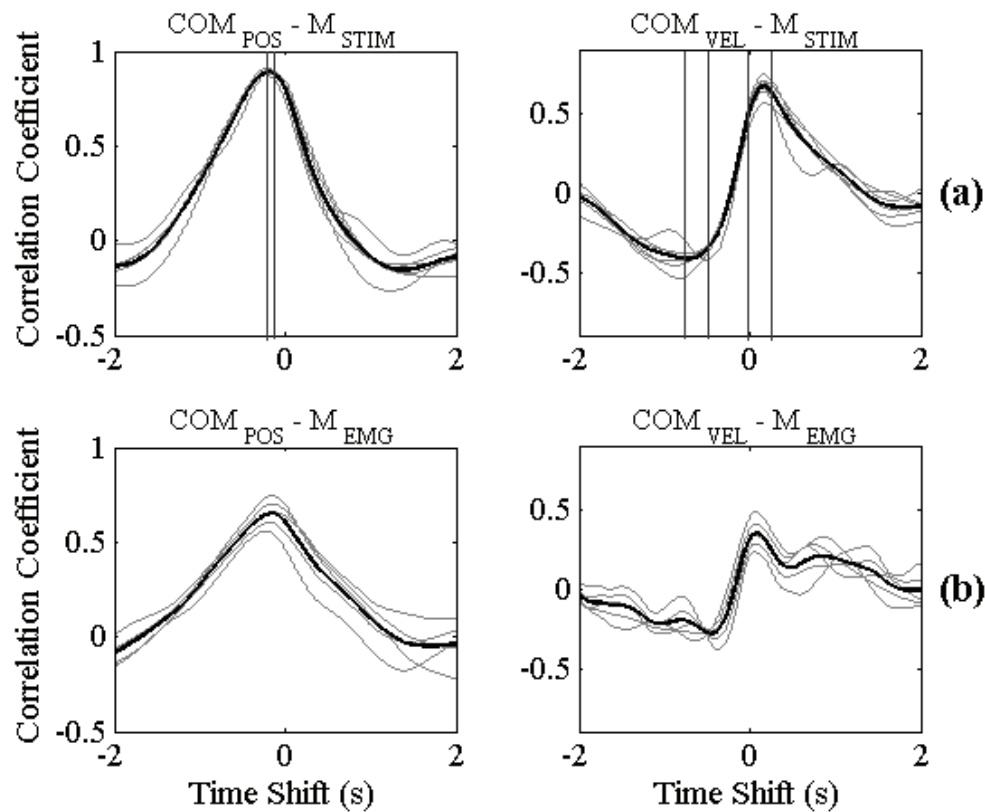


Fig. 4. Cross-correlation comparison: (a) CCFs between  $COM_{POS}$  and  $M_{STIM}$ , and between  $COM_{VEL}$  and  $M_{STIM}$  for the PDstim recordings. The bold black curves indicate the group average CCFs for all six PDstim recordings, whereas the gray vertical lines mark the target ranges for the respective time shifts; (b) CCFs between  $COM_{POS}$  and  $M_{EMG}$ , and between  $COM_{VEL}$  and  $M_{EMG}$  for one able-bodied subject (5 trials of 30 s). Reprinted from (10), with permission from IEEE (© 2007 IEEE).

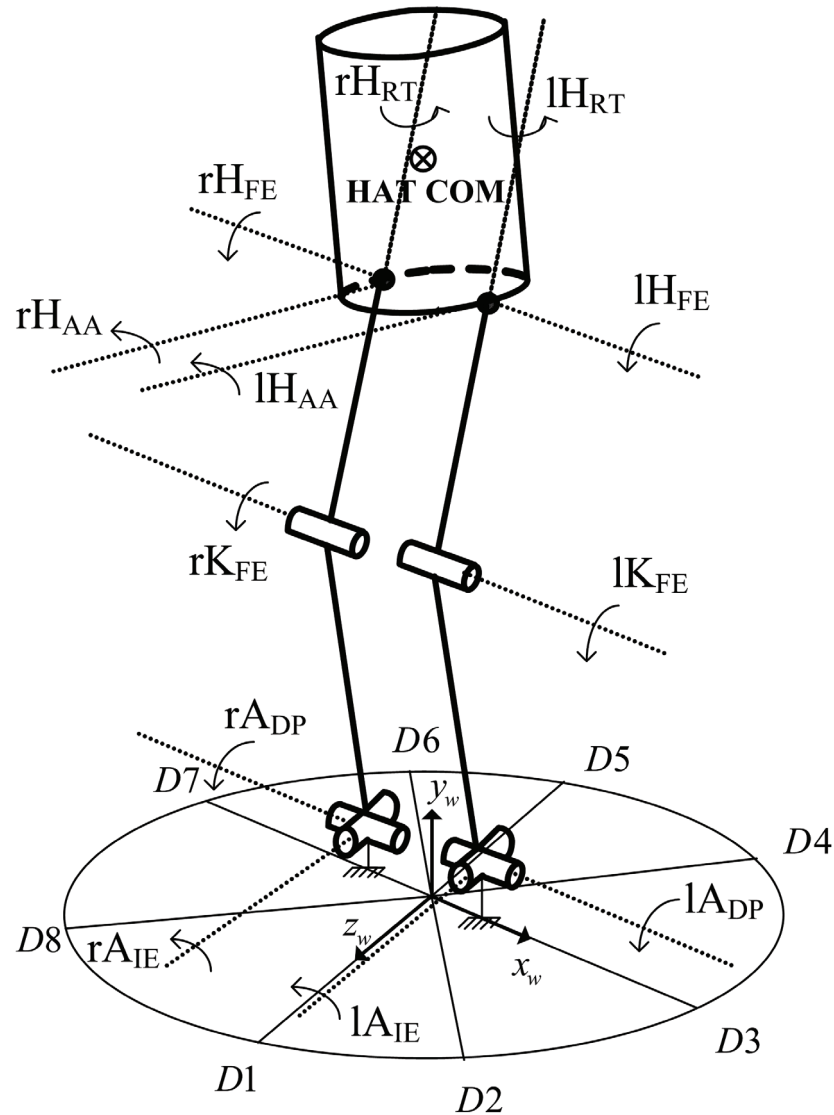


Fig. 5. 3D dynamic model of the human body during double-support stance (12). The DOF of the joints are as follows: ankle inversion/eversion ( $IA_{IE}$ ,  $rA_{IE}$ ); ankle dorsiflexion/plantarflexion ( $IA_{DP}$ ,  $rA_{DP}$ ); knee flexion/extension ( $IK_{FE}$ ,  $rK_{FE}$ ); hip abduction/adduction ( $IH_{AA}$ ,  $rH_{AA}$ ); hip flexion/extension ( $IH_{FE}$ ,  $rH_{FE}$ ); and hip rotation ( $IH_{RT}$ ,  $rH_{RT}$ ). The system was perturbed in eight different directions, D1 to D8. Reprinted from (12), with permission from the American Society of Mechanical Engineers (© 2007 ASME).

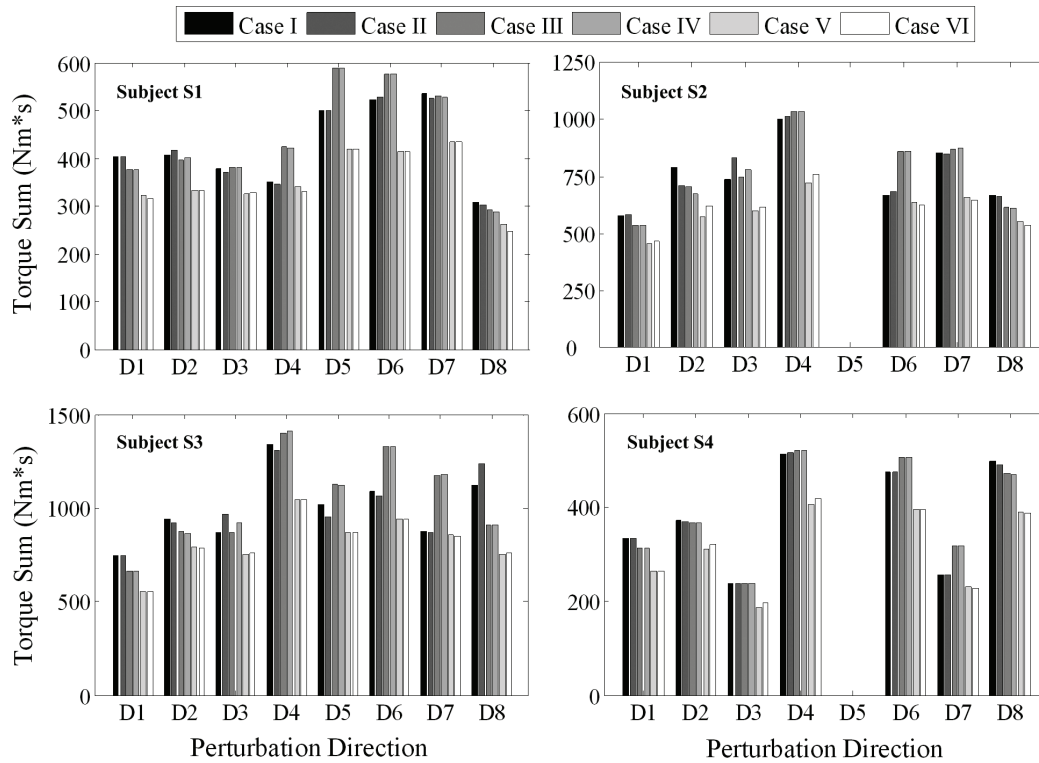
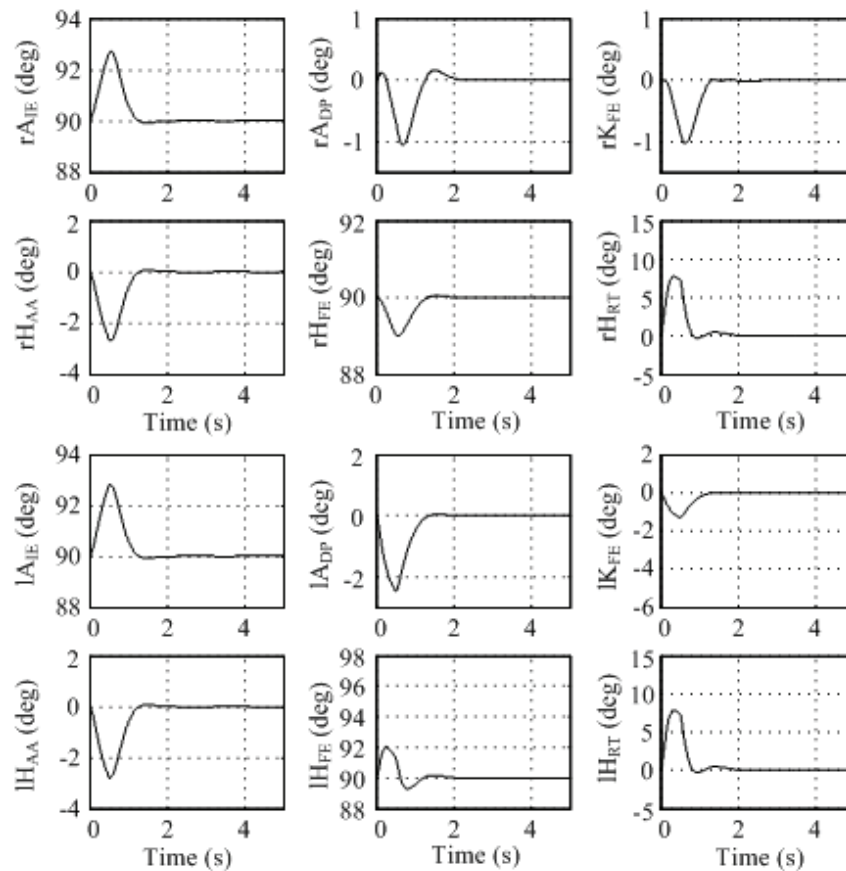
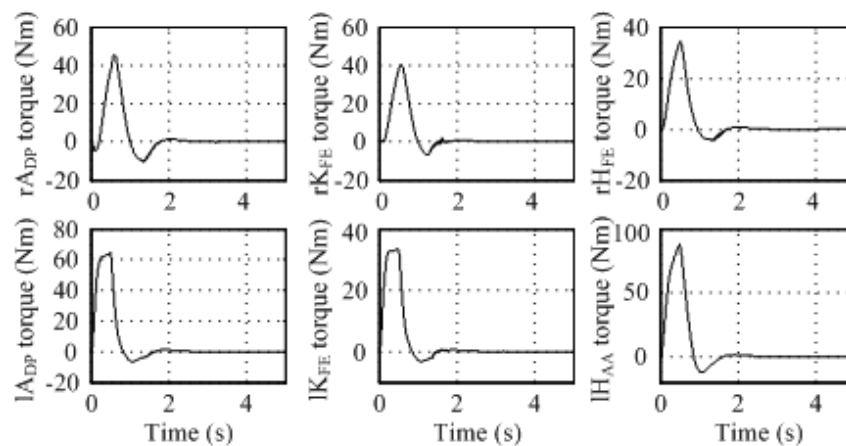


Fig. 6. Torque sums of the joint torques at all active DOF, shown for each of the six 6-DOF systems (Cases I to VI) and all directions of perturbation (D1 to D8). Note that subjects S2 and S4 show overall torque sums for seven perturbation directions only as these subjects lost balance during the D5 perturbations. Reprinted from (12), with permission from ASME (© 2007 ASME).



(a) Joint variable trajectories



(b) Control torque at active DOF

Fig. 7. Simulation results for the PD plus gravity compensator: (a) Joint angles and (b) control torques at the active DOF of Case VI, generated by the PD plus gravity compensator during the perturbation of the 3D dynamic model. Reprinted from (11), with permission from IEEE (© 2006 IEEE).